Experimental Verification of the Physics and Structure of the Bipolar Junction Transistor

I. Mártil, *Member, IEEE*, J. M. Martín, S. García, and G. González-Díaz

***Abstract*— We present an electrical characterization of discrete Bipolar Junction Transistor (BJT) devices with nonuniform doped emitter and base zones. The measurement of the I–V and C–V characteristics of the emitter–base and the collector–base junctions and the common emitter current gain allows to determine relevant parameters of the device. These are the built-in voltage of both junctions, the impurity gradient profiles, the electrical area of both junctions, the base and the emitter Gummel numbers, and the collector doping. The whole experiment can be conducted in a laboratory session of 3–4-hour length and it is specifically addressed to students taking lectures in semiconductor device physics. The results obtained give a deep insight into both the physical structure and the physical processes involved in the transistor behavior.**

***Index Terms*—Bipolar junction transistor, device parameters, physics of BJT's.**

I. Introduction

Bipolar junction transistors (BJT), together with field-effect transistors (JFET, MOSFET, etc.) are the most widely known semiconductor devices. Students of semiconductor device physics devote several weeks to understand the complex physical processes involved in the transistor action. There are excellent books which provide a comprehensive treatment of the physics of both BJT and FET's [1]–[3].

From the practical point of view, laboratory experiments with BJT's are mainly concerned with two aspects: determination of the equivalent circuit of the BJT [4] and simulation of the BJT behavior with proper programs, PSPICE being the most popular among them [5].

However, experiments with the BJT are scarce, and mainly focused on the practical applications of the device (i.e., signal amplification, phase shift, etc.). The electrical characterization of a BJT has been used to obtain information about semiconductor parameters (bandgap of Si and Ge) [6], with no emphasis in the determination of device parameters like doping levels, minority-carrier lifetimes, etc. Quite accurate information about the physical structure of the BJT can be deduced by means of the I–V characteristics of the device starting from the Ebers–Moll model [7] and introducing simple changes into the equations for a more suitable description of double diffused transistors [2]. On the other hand, by means of C–V measurements, it is possible to obtain additional data from the device. However, these experiments can be found only in research papers published during the last thirty years (see, for instance, [1, Ch. 3] and references, therein). From an educational point of view, we have not found undergraduate-level laboratory experiments focused on the practical demonstrations of the main aspects of the BJT theory.

In this paper, we propose a set of electrical measurements to be performed on discrete Si BJT's to measure several key device parameters, which are responsible for the transistor action. The measurements are designed to be done in a 3–4-hour laboratory session and are focused on a second course on semiconductor device physics.

II. Theory

Present-day discrete Si BJT devices are made using the same fabrication processes involved in integrated circuit fabrication. As a consequence, the structure of BJT commercial devices is more complex than the ideal structure: the doping of the base and the emitter zones is made by diffusion or ion implantation of impurities into the uniformly doped collector zone. This means that doping profiles of both the emitter and the base are not uniform and, therefore, it is necessary to use Gummel numbers to characterize their respective doping levels instead of impurity-concentration values [8]. Due to the resulting doping profiles of the three zones, the characteristics of both emitter–base and collector–base junctions (EBJ and CBJ) are dependent on the bias-voltage range of measurement, behaving as linearly graded junctions for small dc bias voltages (both of them) and as an abrupt junction for large reverse dc bias voltages (the CBJ) [2]. In Fig. 1 we present a scheme of the physical structure and the impurity doping profiles for a typical n-p-n BJT double-diffused discrete device [3].

The I–V characteristic of the EBJ, when the collector is short-circuited to the base (i.e., when the BJT works in the so-called transdiode regime where $V_{CB} = 0$) [6], can be written as follows:

$$I_E = qA_E n_i^2 \left(\frac{1}{G_E} + \frac{1}{G_B}\right)(e^{qV_E/kT} - 1) + I_{RE} \quad (1)$$

where V_E is the EBJ dc bias, A_E is the EBJ area, and n_i is the intrinsic Si carrier concentration. G_B and G_E are, respectively, the base and emitter Gummel numbers, defined as follows [3], [9]:

$$G_B = \int_0^{W_B} \frac{N_B(x)}{D_B(x)}\, dx \quad (2)$$

Manuscript received November 13, 1994; revised March 21, 1998.

The authors are with the Departamento Electricidad y Electrónica, Fac. Físicas, Universidad Complutense de Madrid, 28040 Madrid, Spain (e-mail: imartil@eucmax.sim.ucm.es).

Publisher Item Identifier S 0018-9359(98)05719-7.

0018–9359/98$10.00 © 1998 IEEE

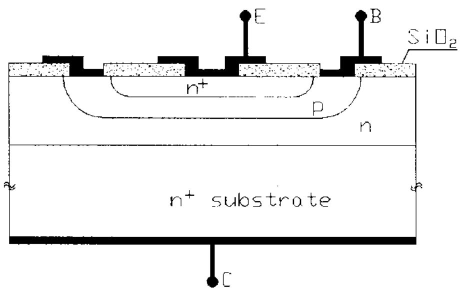

(a)

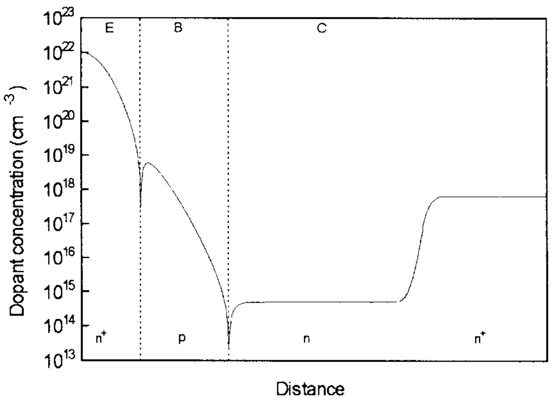

(b)

Fig. 1. (a) Schematic cross section of a discrete BJT. (b) Typical doping profiles: nonuniform emitter, nonuniform base, and epitaxial uniformly doped collector.

$$G_E = \int_0^{W_E} \frac{N_E(x)}{D_E(x)}\,dx \tag{3}$$

where W_E and W_B are the emitter and base widths, respectively, and D_E and D_B are the diffusion coefficients of minority carriers in each zone. G_E and G_B characterize the doping in the respective zones.

The Gummel numbers G_B and G_E determine the dc common emitter current gain of the device, h_{FE}

$$h_{FE} = \frac{G_E}{G_B}. \tag{4}$$

In (1), I_{RE} takes into account the recombination currents in the space-charge zone of the EBJ, and can be written as [10]

$$I_{RE} = \frac{qA_E n_i W}{\tau_r}\,(e^{qV_E/2kT} - 1) \tag{5}$$

where τ_r is the carrier recombination lifetime and W is the width of space-charge zone. The I–V characteristic of the EBJ can be influenced by other nonideal effects, like high injection current from the emitter into the base, base resistance, or both.

Due to the commonly used doping procedures, the capacitive behavior of the EBJ is as in a linearly graded junction. The equation that fully describes it is [1]

$$C_{EB0} = \left(\frac{A_E^3 q\epsilon^2 a_E}{12(V_{bi,\,E} - V_E)}\right)^{1/3} \tag{6}$$

where C_{EB0} is the emitter–base capacitance when the collector is open, a_E is the impurity gradient factor, and $V_{bi,\,E}$ is the built-in voltage of the EBJ.

Regarding the CBJ, if the emitter is short-circuited to the base ($V_{EB} = 0$), the I–V characteristic of this junction is as follows [2]:

$$I_C = qA_C n_i^2\left(\frac{1}{G_B} + \frac{W_C}{N_C\tau_C}\right)(e^{qV_C/kT} - 1) + I_{RC} \tag{7}$$

where V_C is the applied dc bias to the CBJ, A_C is the CBJ area (due to crowding and other doping related effects, A_C is always greater than the EBJ area, A_E), W_C is the uniformly doped collector width, N_C is the collector doping, and τ_C is the minority-carrier lifetime. The collector contribution to the total current $(W_C/N_C\tau_C)$ is negligible in relation with the base contribution $(1/G_B)$, so the I-V characteristic of the CBJ, in the diffusion-dominant regime, can be used to determine the Gummel base number if the collector area A_C is known [8].

As in the case of the EBJ, I_{RC} takes into account the recombination currents in the CBJ space-charge zone and can be written as in (5). Departures from (7) arise from the presence of base resistance, collector resistance, or both.

The capacitive behavior of the CBJ is strongly influenced by the doping profile of both base and collector: it behaves like a linearly graded-type in the low reverse-low forward dc bias voltage range, while at large dc reverse bias the space-charge zone is well inside the uniformly doped collector and the C-V characteristic is as in an abrupt junction.

III. Experimental

We have characterized ten units of the n-p-n 2N2222A general-purpose Si BJT from different manufacturers, five devices with TO-92 plastic encapsulation type (from ITT), and five other with TO-18 metallic encapsulation (from Motorola). In performing the measurements, we discovered that the TO-18 encapsulated devices showed an anomalous behavior in the CBJ I–V characteristic, with unexpected, very high current values in the 0–0.4-V range. For voltages higher than 0.4 V, the I–V characteristic was roughly the expected one. We think that surface or leakage currents, strongly dependent on the encapsulation type, may be the reason for such anomalous behavior. Due to this fact, we will present only the results obtained with the TO-92 devices.

Following the theory outlined in the previous section, the I–V characteristics of both EBJ and CBJ were obtained with the third terminal short-circuited to the base. The measurements were made following a procedure already described in a previous paper devoted to p-n junction characterization [11]. We will briefly describe it here: in the 10^{-12}–10^{-5}-A current range, the measurements were obtained using a Keithley K-602 electrometer ($R_i = 10^{12}\ \Omega$) in the ohmmeter configuration, in which the electrometer works as a current supply, injecting into the p-n junction a current whose value is the inverse of the ohmmeter scale reading, and the meter reading gives the device voltage drop across the junction. In this way, a single set of current–voltage values is obtained for each ohmmeter range. In the 10^{-5}–10^{-1}-A current range, we measured the I–V characteristics by using an external current supply, with the electrometer now used as a high-impedance voltmeter, and

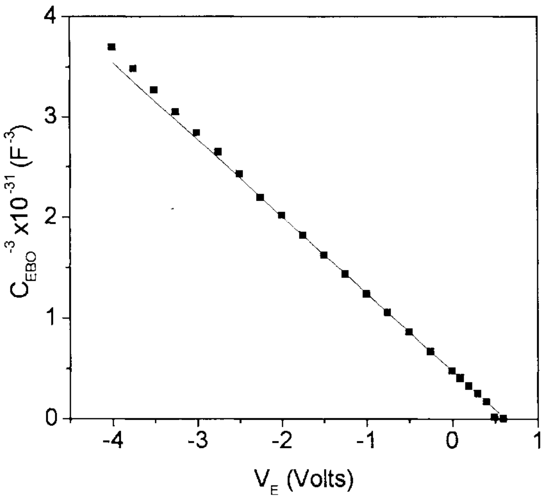

Fig. 2. C_{EB0}^{-3} as a function of dc bias voltage V_E for a representative device with plastic encapsulation (TO-92).

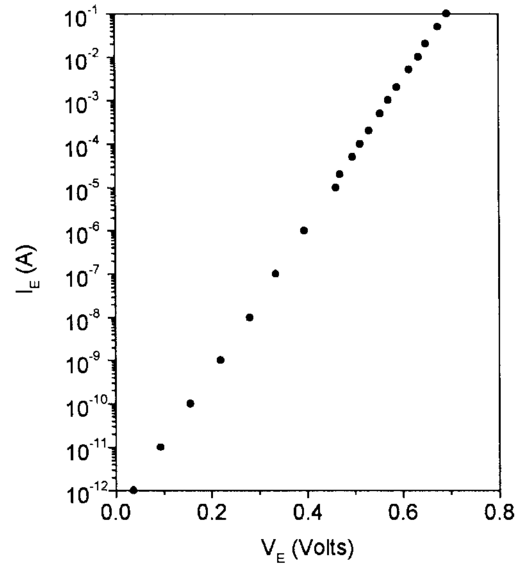

Fig. 3. I–V characteristic of the EBJ in the transdidode configuration ($V_{CB} = 0$) for the same device of Fig. 2.

we measured the current values with a digital multimeter. In this range, we have measured three experimental points per current decade. With this experimental setup, it is possible to obtain very accurate values of the reverse diffusion and recombination saturation currents (the estimated error is lower than 2%). This precision was good enough to obtain the right values of the Gummel numbers.

The C–V characterization was done by measuring the $C_p - G_p$ small-signal equivalent circuit of both the EBJ and CBJ with the third terminal open (i.e., we measured C_{EB0} and C_{CBO} capacitances, respectively) with an HP-4284A impedance analyzer. The dc bias ranged between -10 and 0.6 V. In the -10–0-V range, ac small-signal bias was 50 mV, while in the 0–0.6-V range, it was 15 mV. These conditions were found to be the best choice to obtain both capacitance and conductance values with a precision better than 10^{-2} pF and 10^{-3} μS, respectively, over the whole range of measurements [12]. We present only measurements taken at $f = 1$ MHz. Measurements performed at lower frequencies (1, 10, and 100 kHz) gave the same results. The accurate determination of the capacitance is also necessary to obtain the right values of the emitter and the collector areas (errors less than 10%).

The common emitter output characteristics were measured with a Tektronics 571 curve tracer to obtain the dc common emitter current gain parameter, h_{FE} (the estimated error for this parameter is 4%).

IV. Results and Discussion

We present results of EBJ and CBJ separately. For each junction we first present the results of the C–V measurements.

A. Emitter–Base Junction

In Fig. 2, we plot C_{EB0}^{-3} data as a function of dc reverse bias for a representative device. From the plot, a straight line in the -3- to -0.5-V dc bias range can be seen. As expected from a double-diffused junction, this behaves as a linearly graded one, in agreement with (6). From the extrapolation to $C_{EB0}^{-3} = 0$, we obtain the built-in voltage of the EBJ, $V_{bi,\,E}$. The impurity gradient factor a_E is obtained from the relation between the built-in voltage and a_E [13]

$$V_{bi,\,E} = \frac{2}{3}\,\frac{kT}{q}\,\ln\left(\frac{a_E^2 \epsilon kT/q}{8qn_i^3}\right) \tag{8}$$

where the built-in voltage is the so-called "gradient" voltage.

Thus from the C–V measurements, we obtain the following values for the different junction parameters involved in (6) and (8):

$$\begin{aligned} V_{bi,\,E} &= 0.62 \pm 0.01 \text{ V} \\ a_E &= (9 \pm 2) \times 10^{20} \text{ cm}^{-4} \\ A_E &= (2.1 \pm 0.2) \times 10^{-3} \text{ cm}^2. \end{aligned}$$

As noted by Chawla and Gummel [13], the use of the built-in voltage as in (8) (the "gradient" voltage) is mandatory to obtain an accurate value of the impurity gradient a_E and, hence, of the EBJ electrical area A_E. For the studied devices we have found with an optical microscope that the physical area of the BJT is $(3.6 \pm 0.4) \times 10^{-3}$ cm^2. However, the device topography is an interdigitated complex structure and thus it was not possible for us to measure the actual EBJ or CBJ area. It should be pointed out that if the experimental data are analyzed in the usual framework of linearly graded junctions [1]–[3], unrealistic values are obtained for the parameters quoted above. This important question has been extensively analyzed by Van den Biesen in two papers [14] and [15]. For the purpose of our experiment, the "gradient" voltage approximation for $V_{bi,\,E}$ quoted in (8) gives a simple and excellent quantitative treatment of the C–V data.

Fig. 3 shows the I–V characteristic of the EBJ for the same device as that of Fig. 2. It can be seen that over the ten orders of magnitude of current measured, the characteristic fit well to the diffusion current (1). In the 10^{-11}–10^{-8}-A range, there is a slight departure from the ideal behavior, due to the presence of recombination currents in the space-charge zone of the EBJ, accounted for by I_{RE} in (1). The fitting in the ideal regime

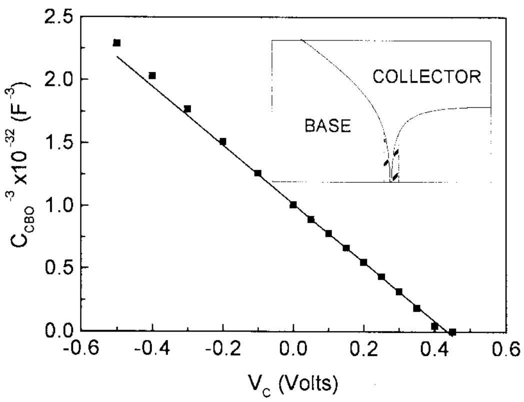

(a)

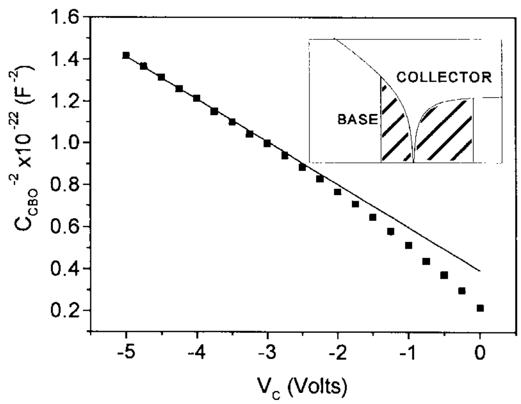

(b)

Fig. 4. (a) C_{CB0}^{-3} as a function of dc bias voltage V_C, of the device of Figs. 2 and 3. The inset shows the space-charge distribution, were the CBJ behaves as a graded junction. (b) C_{CB0}^{-2} as a function of reverse dc bias voltage V_C for the same device. The inset shows the transition from graded to abrupt nature for this junction.

gives a saturation current of $(2.39 \pm 0.04) \times 10^{-14}$ A. From the output common emitter characteristics measured, we obtain the common emitter current gain $h_{FE} = 220 \pm 10$.

We now determine the Gummel number of the base G_B as follows: we introduce the h_{FE} value into (4), then substitute it in the expression for the diffusion reverse saturation current quoted in the first term of (1), and using the emitter area, A_E deduced from the C–V measurements, we finally obtain

$$G_B = (3.6 \pm 0.5) \times 10^{11}\ \text{cm}^{-4} \cdot \text{S}.$$

This is a typical value for the base Gummel number in double-diffused silicon transistors [9]. We will again determine G_B from the I–V characteristic of the CBJ in Section IV-B.

We now obtain the emitter Gummel number G_E from (4)

$$G_E = (7.9 \pm 1.5) \times 10^{13}\ \text{cm}^{-4} \cdot \text{s}$$

also a typical value for this parameter [9].

B. Collector–Base Junction

In Fig. 4(a), we plot C_{CB0}^{-3} as a function of the dc bias voltage for the same device as before. In the -0.5- to 0.5-V range, the data fit well to a straight line, showing the graded character of the CBJ in this range. For dc bias voltage lower than -3 V, the data fit to a C_{CB0}^{-2} behavior, thus indicating the change from graded to abrupt for the CBJ, already described for diffused junctions. Fig. 4(b) is a plot of C_{CB0}^{-2} versus dc bias. Inset into both Fig. 4(a) and (b) is a picture that graphically illustrates the transition from graded to abrupt CBJ.

The analysis of the data of Fig. 4(a) is as it was done with Fig. 2 for the EBJ and gives us the following value for the junction parameters:

$$\begin{aligned} V_{bi,C} &= 0.44 \pm 0.01\ \text{V} \\ a_C &= (4 \pm 1) \times 10^{18}\ \text{cm}^{-4} \\ A_C &= (4.1 \pm 0.4) \times 10^{-3}\ \text{cm}^2. \end{aligned}$$

The “gradient” voltage and the impurity gradient parameter are lower than those obtained for the EBJ, as expected from a double-diffused junction [2]. Collector area is greater than emitter area, due to divergent paths for the emitter-to-collector current (i.e., the crowding effect at the emitter-to-base contact). The collector area is also quite similar to the device area, which is consistent with the physical structure of a discrete device, where the collector contact is made in the back of the BJT, in the whole chip area [3].

We determine the doping level of the epitaxial collector zone, N_C, by means of the data of Fig. 4(b). In fact, from the theory of the unilateral abrupt junction it is easy to show that

$$\frac{dC_{CB0}^{-2}}{dV} = \frac{2}{q\epsilon N_C A_C^2}. \tag{9}$$

From the analysis, a collector doping of $(4 \pm 1) \times 10^{14}$ cm^{-3} is deduced, a common value for this parameter (usually this ranges from 10^{14} to 10^{16} cm^{-3}) [2]. A careful analysis of the experimental data following the graphical procedure described in [13] gives a collector doping of 5×10^{14} cm^{-3}, in good agreement with the above quoted value. Then, the procedure outlined in the previous paragraph gives an accurate and simple way to obtain the collector doping, without the use of troublesome graphical procedures, where the physical meaning is usually not apparent to the students.

In Fig. 5, we plot the I–V characteristics of the CBJ for the same device. The fitting of the data of Fig. 5 to (7), gives a reverse saturation current of $(3.8 \pm 0.05) \times 10^{-13}$ A. As before, using the expression for this current and the collector area deduced from C–V measurements, we determine the base Gummel number G_B

$$G_B = (3.9 \pm 0.6) \times 10^{11}\ \text{cm}^{-4} \cdot\ \text{s}$$

in quite good agreement with the previously determined value from the I–V and C–V data of the EBJ.

Finally, Fig. 5 shows an obvious departure from (7) in the high-voltage zone probably due to the presence of a collector resistance [1], [2].

V. Conclusions

We have measured the I–V and C–V characteristics of the EBJ and CBJ of Si 2N2222A general-purpose BJT’s, with TO-92 plastic encapsulation. We have also measured the output common emitter characteristics. From the measurements, we

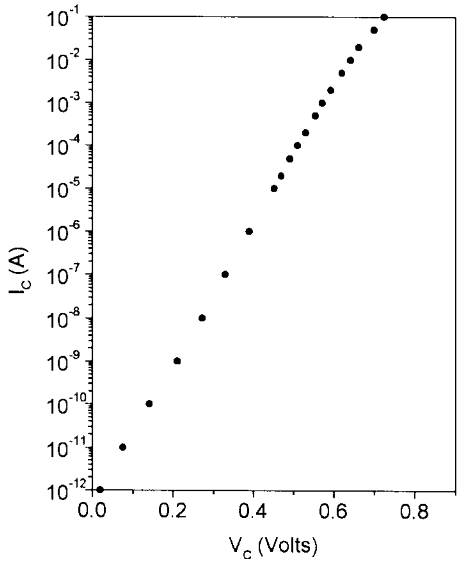

Fig. 5. I–V characteristic for the CBJ in the transdiode configuration $(V_{EB} = 0)$ for the device of Figs. 2–4.

obtain the following values of the relevant parameters of the device:

Geometrical parameters:

$$A_E = (2.1 \pm 0.2) \times 10^{-3} \text{ cm}^2$$
$$A_C = (4.1 \pm 0.4) \times 10^{-3} \text{ cm}^2.$$

Impurity gradient parameters:

$$a_E = (9 \pm 2) \times 10^{20} \text{ cm}^{-4}$$
$$a_C = (4 \pm 1) \times 10^{18} \text{ cm}^{-4}.$$

Doping parameters:

$$G_B = (3.6 \pm 0.5) \times 10^{11} \text{ cm}^{-4} \text{ s}$$
$$G_E = (7.9 \pm 1.5) \times 10^{13} \text{ cm}^{-4} \text{ s}$$
$$N_C = (4 \pm 1) \times 10^{14} \text{ cm}^{-3}.$$

The results allow us to confirm the graded character of the EBJ. The analysis of CBJ also confirm the graded character of this junction at low dc bias voltage and its abrupt behavior at large reverse-bias voltage. The whole experiment gives a valuable procedure to obtain an accurate picture of the physical structure of present-day BJT Si discrete devices. The experiment showed in this paper may be performed in a laboratory session of 3–4 hours long, and is specifically addressed to students taking lectures in a second-level semiconductor device physics course.

References

[1] S. M. Sze, *Physics of Semiconductor Devices,* 2nd ed. New York: Wiley, 1981, pp. 133–156.

[2] D. J. Roulston, *Bipolar Semiconductor Devices.* New York: McGraw-Hill, 1990, pp. 178–181, 212–220, and 226–229.

[3] M. S. Tyagi, *Introduction to Semiconductor Materials and Devices.* New York: Wiley, 1991, pp. 385–398 and 414–418.

[4] S. Natarajan, "An effective approach to obtain model parameters for BJTS and FETS from data books," *IEEE Trans. Educ.*, vol. 35, pp. 164–169, 1992.

[5] N. R. Malik, "Determining SPICE parameter values for BJT's," *IEEE Trans. Educ.*, vol. 33, pp. 366–368, 1990.

[6] A. Sconza, G. Torzo, and G. Viola, "Experiment on the physics of the PN junction," *Amer. J. Phys.*, vol. 62, pp. 66–70, 1994.

[7] J. J. Ebers and J. L. Moll, "Large-signal behavior of junction transistors," *Proc. IRE*, vol. 42, pp. 1761–1772, 1954.

[8] H. K. Gummel, "Measurements of the number of impurities in the base layer of a transistor," *Proc. IRE*, vol. 49, p. 834, 1961.

[9] D. L. Pulfrey and N. Garry Tarr, *Introduction to Microelectronic Devices.* Englewood Cliffs, NJ: Prentice-Hall, 1989, pp. 366–367.

[10] C. T. Sah, R. N. Noyce, and W. Shockley, "Carrier generation and recombination in pn junction and pn junction characteristics," *Proc. IRE*, vol. 45, pp. 1228–1243, 1957.

[11] I. Mártil and G. González-Díaz, "A laboratory experiment for DC characterization of PN devices," *Eur. J. Phys.*, vol. 12, pp. 148–152, 1991.

[12] M. L. Lucía, J. L. Hernández-Rojas, C. León, and I. Mártil, "Capacitance measurements on pn junctions: Depletion layer and diffusion capacitance contributions," *Eur. J. Phys.*, vol. 14, pp. 86–89, 1993.

[13] B. R. Chawla and H. K. Gummel, "Transition region capacitance of diffused pn junctions," *IEEE Trans. Electron Devices* vol. ED-18, pp. 178–195, 1971.

[14] J. J. H. Van den Biesen, "P-N junction capacitances. Part I: The depletion capacitance," *Phillips J. Res.*, vol. 40, pp. 88–102, 1985.

[15] ——, "P-N junction capacitances. Part II: The neutral capacitance," *Phillips J. Res.*, vol. 40, pp. 103–113, 1985.

I. Mártil (M'88) was born in Madrid, Spain, in 1956. He received the degree in physics from the Universidad Complutense de Madrid in 1978 and the Ph.D. degree from the same university in 1982.

From 1980 to 1991, he worked on polycrystalline semiconductors and heterojunction devices for photovoltaic applications. After 1991, he worked on III–V compound semiconductor devices, with his main research activities now InP-based MISFET devices. Preseently, he is an Assistant Professor in the Department of Electronics, Physics Faculty, at Universidad Complutense de Madrid. He has authored or coauthored more than 50 research papers on international journals and conference articles and more than ten educational papers on the physics of semiconductor devices such as p-n junction, solar cells, light-emitting diodes, and semiconductor lasers.

J. M. Martín received the degree in physics in 1990 and the Ph.D. degree in 1995, both from the Universidad Complutense de Madrid, Spain.

He is currently with Lucent Technologies, Tres Cantos, Madrid, working as Development Engineer. He has authored or coauthored more than 20 papers in international journals on electrical and optical characterization of ion-implanted InP wafers and on the electrical characteristics of InP-based p-n junctions.

In 1997, Dr. Martin received the award for young researches of the R.S.E.F (Spanish Royal Society of Physics).

S. García received the degree in physics in 1991 and the Ph.D. degree in 1996, both from the Universidad Complutense de Madrid, Spain.

He is currently with Lucent Technologies, Tres Cantos, Madrid, working as Development Engineer. He has authored or coauthored more than 15 papers in international journals on the properties of $SiN_x:H$ films deposited by ECR-CVD plasma-deposition process and on electrical characterization of metal–insulator–semiconductor structures.

G. González-Díaz was born in Valladolid, Spain, in 1952. He received the degree in physics from the Universidad de Valladolid in 1974 and the Ph.D. degree from the Universidad Complutense de Madrid, Spain in 1979.

He is Professor at the Department of Electronics, Physics Faculty, Universidad Complutense de Madrid and Deputy Dean and Director of the Ion Implantation Facility at this University. He has authored or coauthored more than 60 research papers in international journals and as conference articles.